Organic Electronics 14 (2013) 187–192

Contents lists available at SciVerse ScienceDirect

Organic Electronics

journal homepage: www.elsevier.com/locate/orgel

Improvement of light out-coupling in organic light-emitting diodes by printed nanosized random texture layer

Se Joong Shin [a], Tae Hyun Park [a], Jin Hwan Choi [a], Eun Ho Song [a], Hakkoo Kim [a], Hyun Jun Lee [a], Jeong-Ik Lee [b], Hye Yong Chu [b], Kyu Back Lee [c], Young Wook Park [d,*], Byeong-Kwon Ju [a,*]

[a] Display and Nanosystem Laboratory, College of Engineering, Korea University, Seoul 136-713, Republic of Korea
[b] Convergence Components and Materials Research Laboratory, Electronics and Telecommunications Research Institute, Daejeon 305-350, Republic of Korea
[c] Department of Biomedical Engineering, College of Health Science, Korea University, Seoul 136-713, Republic of Korea
[d] The Institute of High Technology Materials and Devices, Korea University, Seoul 136-713, Republic of Korea

ARTICLE INFO

Article history:
Received 31 May 2012
Received in revised form 4 October 2012
Accepted 12 October 2012
Available online 9 November 2012

Keywords:
Organic light-emitting diodes (OLEDs)
Nanosized structures
Random pattern
Out-coupling
Printing process

ABSTRACT

We demonstrate greatly improved light out-coupling efficiency and undistorted light output in organic light-emitting diodes (OLEDs) containing a nanosized random texture layer (nRTL). The nRTL is fabricated on a glass substrate by an inexpensive and simple printing process. Compared to a conventional device, OLEDs with the nRTL showed greatly improved power efficiency (+102%) at a luminance of 3000 cd/m^2. The nRTL is free of viewing-angle-dependent color and brightness distortion and suitable for industrial mass production.

1. Introduction

Organic light-emitting diodes (OLEDs) have been successfully employed as flat panel displays; [1–2] their use in TVs and as solid-state light sources is being actively investigated [3–5]. Great progress has been made recently in improving their luminous efficiency, device lifetime, and color gamut. However, commercially available OLEDs still lack these enhancements. Although the conversion efficiency of injected electrons into photons has reached almost 100% [6], there is still considerable room for improving the light extraction efficiency. However, almost 80% of the generated light is lost because of wave-guiding and total internal reflection at the indium tin oxide (ITO)/glass substrate and glass substrate/air interfaces. Thus, only about 20% of the generated photons leave the device as useful light [7–9]. This low out-coupling efficiency reduces the OLED lifetime because the driving voltage must be increased in order to achieve the desired brightness. Therefore, efforts have been made to extract the light from the device in guided modes. Various methods have been reported to increase the out-coupling efficiency, including the use of substrate surface texturing [10], periodic photonic crystal (PC) structure [11–15], a thin silica aerogel layer [16], and a low-index grid [17]. In addition, extraction can be improved by modifying the glass substrate/air interface with a micro-lens array [18–20] or sandblasted surfaces, or by meshing the glass substrate modes [21]. However, most of these methods require complicated, costly fabrication procedures and yield limited enhancement, distorted or shifted output spectra [13], and a limited aperture ratio [15]. Therefore, it is still necessary to develop a method of enhancing the out-coupling efficiency without these drawbacks in order to fabricate efficient OLEDs, especially for use in flat panel light sources. Although PC structures improve the light extraction with a high aperture

* Corresponding authors.
E-mail addresses: zerook@korea.ac.kr (Y.W. Park), bkju@korea.ac.kr (B.-K. Ju).

1566-1199/$ - see front matter © 2012 Elsevier B.V. All rights reserved.
http://dx.doi.org/10.1016/j.orgel.2012.10.009

ratio and allow for simple fabrication [11,12,14], the light emitted by periodical PC OLEDs is strongly distorted depending on the viewing angle owing to diffraction of light by the PC structures [13]. Thus, this method is not suitable for fabrication of OLED flat panel light sources. The structures have been arranged in random positions to remove the viewing-angle-dependent color distortion. For example, Takezoe's group reported that a buckled structure with directional randomness obtained by using spontaneously formed buckles improved the light out-coupling without spectral changes [22]. This approach has promise as a light out-coupling enhancement technology for OLEDs. However, the spontaneously formed buckles are difficult to apply reproduction on a large area. Because this is a complex process, it is difficult to apply in practical mass production.

Here, we present a new method that overcomes these significant drawbacks, offering high reproducibility and large-area application by using low-cost printing technology.

A light out-coupling enhancement structure, the nanosized random texture layer (nRTL), is fabricated between the transparent anode and the glass substrate using economical, simple printing of a simply fabricated nanostructured stamp on a transparent photoresist (SU-8). OLEDs containing the nRTL demonstrated greatly improved electroluminescence (EL) characteristics compared to a reference device at the same current density. In addition, the printed nRTL showed no viewing-angle-dependent distortion in the emitted light.

2. Experimental

The nRTL was fabricated by a simple method consisting of two-step reactive ion etching (RIE) by oxygen (O_2) and trifluoromethane (CHF_3) gases [23,24] and a low-cost printing process. Fig. 1 shows the process flow of the printed nRTL.

The fabrication of the master began with a quartz substrate. First, the quartz was cleaned in an ultrasonic bath with acetone, methanol, and deionized water for 15 min. It was then dried in an oven at 120 °C. Poly(methyl methacrylate) (PMMA, Micro Chem Co.) was used as the etching mask for the random pattern. The PMMA was spin-coated on the quartz and then annealed on a hot plate (Fig. 1a). Next, the quartz was dry-etched by RIE in order to produce randomly dispersed nanosized structures having a parabolic shape [23,24] (Fig. 1b and c). Fig. 2a presents a three-dimensional atomic force microscopy (AFM) image of the nanosized random structures on the prepared quartz master. The diameters and heights of the structures, as measured by AFM, were around 80–120 nm and 50–80 nm, respectively.

The shape of the quartz master was accurately reproduced on the stamp by the printing process (Fig. 1d and e). The stamp was composed of a thin layer of hard polydimethylsiloxane (h-PDMS, Sylgard Q3-3600 part A and B, Dow Corning) supported by a thick layer of soft PDMS (Sylgard 184 A and B, Dow Corning). A thin layer of h-PDMS was spin-coated onto the quartz master at a speed of 1000 rpm for 40 s and then cured for 10 min at room temperature. The PDMS liquid pre-polymer was poured onto the h-PDMS layer, which was subsequently cured for 2–3 h at 70 °C. Fig. 2b shows an AFM image of the replicates in PDMS/h-PDMS. The composite PDMS/h-PDMS stamp is maximally matched to the greatest degree possible with the randomly patterned master.

The composite stamp was used in the printing process to pattern a highly transparent resin having a refractive index intermediate value between those of the ITO layer (n_{ITO} = 1.8–1.9) and the glass substrate (n_{glass} = 1.5): SU-8 2000.5 (n_{SU-8} = 1.59 @ λ = 520 nm, Micro Chem Co.). The

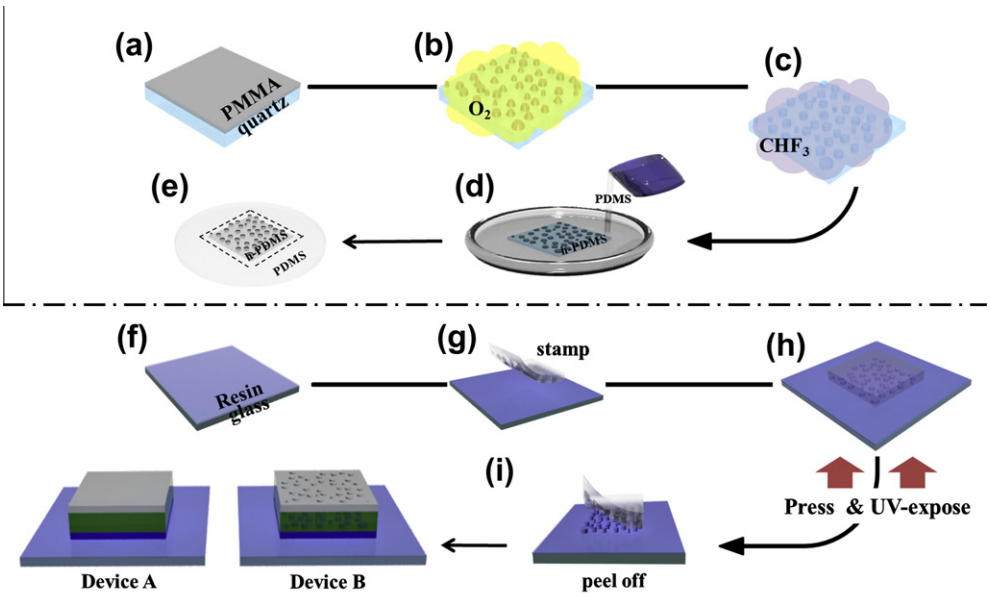

Fig. 1. Schematic illustration of simple printing process for direct fabrication of the nRTL.

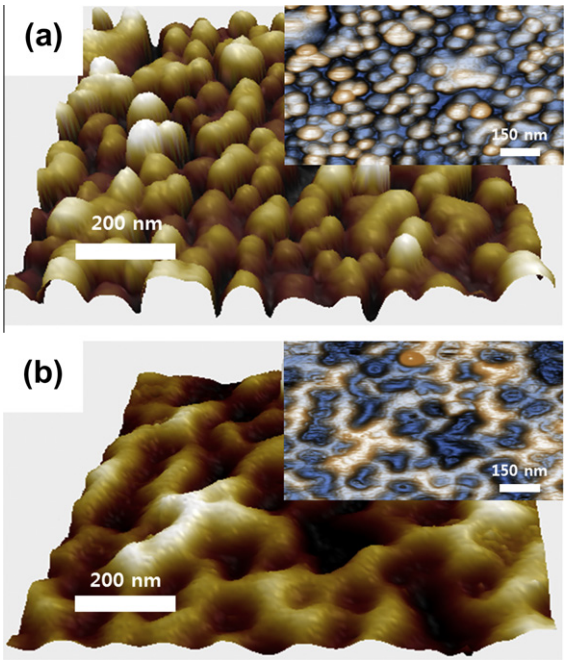

Fig. 2. AFM analysis of nanosized random structures (dimensions: 1000 nm × 1000 nm). (a) Three-dimensional AFM image of quartz master. Diameters and heights of the random structures are around 80–120 nm and 50–80 nm, respectively (inset: two-dimensional AFM image). (b) Three-dimensional AFM image of composite PDMS/h-PDMS stamp. Composite stamp is clearly the negative side of the image on the quartz master (inset: two-dimensional AFM image).

stamp was printed on spin-coated SU-8 on Eagle XG glass at room temperature under an air atmosphere (Fig. 1f and g). The nRTL was formed (Fig. 1h and i) after a few seconds of UV exposure and pressing.

Fig. 3a presents a three-dimensional AFM image of the printed nRTL. The diameters and heights of the nRTL, as measured by AFM, were accurately reproduced from the master to the nRTL. The fabricated nRTL was printed uniformly on the entire light-emitting areas of the devices. Therefore, large areas can be covered with the nRTL, limited only by the size of the quartz master. The nRTL is suitable for practical mass production because this method is capable of high reproducibility and large area application and uses a low-cost printing process. Fig. 3b and c shows the difference in light diffraction between a periodic structure and the random structure. The printed PC structures exhibit a rainbow effect similar to that produced by a prism (Fig. 3b), whereas the nRTL shows no color distortion because light is scattered in random directions by the randomly arrayed nanosized structures (Fig. 3c).

Next, radio frequency sputtering was used to deposit an ITO transparent anode having a thickness of 200 nm and a resistance of 35 Ω/sq. To evaluate the out-coupling efficiency enhancement due to the nRTL, three types of OLEDs were fabricated. Device A contains an SU-8 interlayer produced by spin-coating; device B contains an SU-8 nRTL produced by the printing technique. As a reference device, OLEDs without the nRTL were fabricated. On top of the ITO anodes, OLEDs with an active area of $4 \times 4\ mm^2$ were fabricated by thermal evaporation in a high vacuum ($\sim 2 \times 10^{-6}$ Torr) onto all three substrates simultaneously to ensure consistent results.

Fig. 3d shows the OLED structure, which consisted of a 60 nm thick film of N, N″-bis(naphthalene-1-yl)-N, N″-bis(phenyl)-benzidine (NPB) as a hole–transport layer,

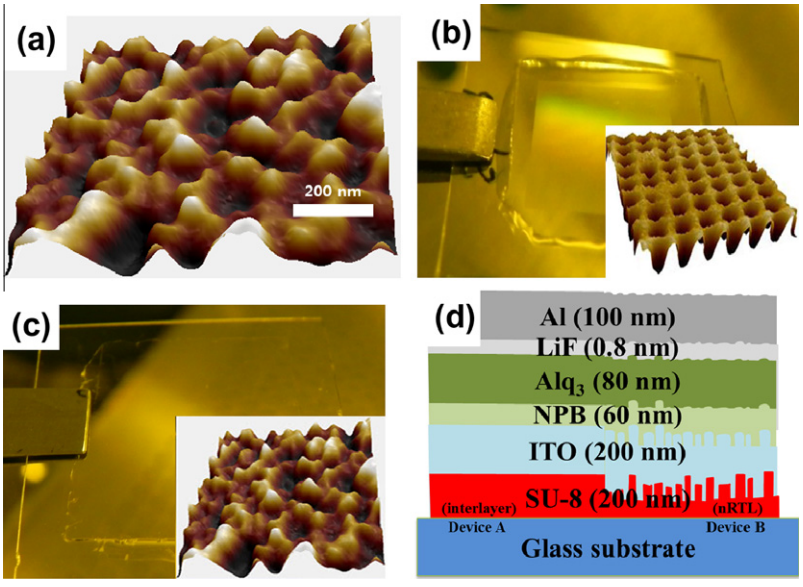

Fig. 3. (a) Three-dimensional AFM image of the nRTL fabricated by a simple printing process. The structure of the random pattern is preserved in the nRTL. The diameters and heights of the nRTL are around 80–120 nm and 50–80 nm, respectively. (b) Image of viewing-angle-dependent color variation caused by periodic pattern (inset: AFM image of tow-dimensional periodic pattern fabricated by printing process, period = 555 nm) and (c) removal of color variation by random pillars (inset: AFM image of random pattern fabricated by printing process; period = randomicity). (d) Schematic of proposed OLED structure with nRTL, where the random corrugated pattern is imprinted on a glass substrate. (For interpretation of the references to colour in this figure legend, the reader is referred to the web version of this article.)

80 nm thick tris(8-hydroxy-quinolinato)aluminum (Alq_3) as an emission layer, 0.8 nm thick lithium fluoride (LiF) as an electron-injection layer, and 100 nm thick aluminum as a cathode. The deposition rates of all of the organic materials and metals were ~1 and ~6 Å/s, respectively. The ITO electrode, organic layer, and aluminum electrode were corrugated because of the nRTL.

The EL characteristics of the fabricated OLEDs were measured by using a high-voltage source measurement unit (Model 237, Keithley Instruments, Inc.) and a spectroradiometer (PR-670 SpectraScan, Photo Research, Inc.).

3. Results and discussion

Fig. 4 shows the EL characteristics of the fabricated OLEDs. Table 1 summarizes their device performance.

Fig. 4a depicts the current density and luminance as a function of the applied voltage.

The operating voltages of device A, which had the interlayer, were similar to those of the reference device. On the other hand, the operating voltages of device B, which had the nRTL, were lower than those of the device A. This performance can be explained by a peculiarity of the ITO/glass interface. The current density is greater at the same bias voltage compared to the reference because the surface area of the electrode is increased by the nRTL. The corrugated OLED structure is well known to reduce the operating voltage [11,19,22].

Moreover, as shown in Fig. 4b, the EL efficiency of the devices with the nRTL is enhanced at the same luminance as a result of the corrugated structure [22]. The power efficiencies of the fabricated devices were 0.82 (device A), 1.10 (device B), and 0.54 lm/W (reference), and the current efficiencies were 3.32, 3.85, and 2.39 cd/A, respectively, at a luminance of 3000 cd/m^2. The power efficiency and current efficiency are enhanced by +51% (device A) and +102% (device B), and +39% (device A) and +61% (device B), respectively. The current and power efficiencies of the OLEDs are summarized in Table 1. This enhanced efficiency in device A can be explained by the reflective index matching effect of the interlayer. Consequently, more of the light trapped at the ITO/glass interface escaped in device A than in the reference device. In device B, the nRTL can enhance the out-coupling efficiency by remixing the trapped light by a scattering mechanism inside the device. Therefore, wave-guided modes can be extracted and coupled out into the glass.

Fig. 4c shows the external quantum efficiency (EQE) as a function of the applied current density. The EQE of the reference device is 0.96% at a current density of 100 mA/cm^2, whereas in devices A and B it is increased by +10% and +48% to 1.05% and 1.42%, respectively. The EQE improvement factor increases with increasing current density. This fact is attributed to the non-uniformity of current injection depending on the surface roughness, which is caused by the absence of a buffer layer on the nRTL and has less effect at high current density. Our research indicates that our method is a simple, low-cost technique for improving the power efficiency of OLEDs, although the structure has not

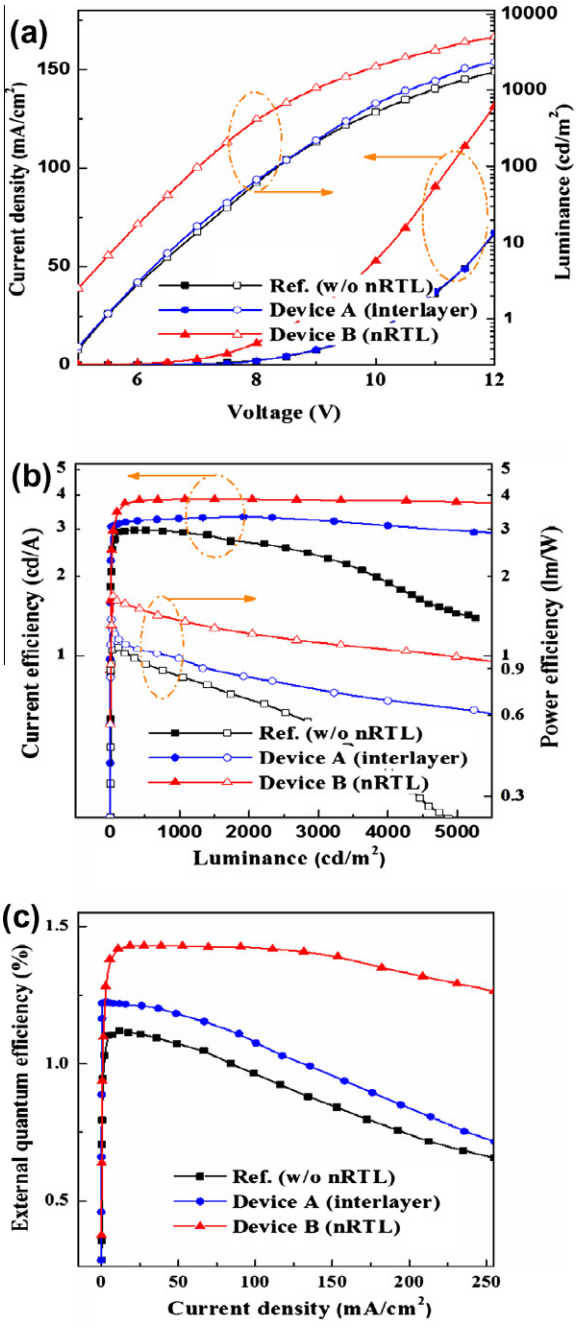

Fig. 4. (a) Current density–luminance–voltage characteristics of conventional OLEDs without the nRTL (squares), device A with interlayer (circles), and device B with the nRTL (triangles). Solid and open symbols represent the current density and luminance of the devices, respectively. (b) Current efficiency and power efficiency as a function of luminance for typical OLEDs without the nRTL (squares), device A with interlayer (circles), and device B with the nRTL (triangles). Solid and open symbols represent the current efficiency and power efficiency, respectively, which were improved by +39% and +51% in device A and +61% and +102% in device B, respectively, at a luminance of 3000 cd/m^2. (c) EQE–current density characteristics of conventional OLEDs without the nRTL (squares), device A with interlayer (circles), and device B with the nRTL (triangles). The EQE values of devices A and B at a current density of 100 mA/cm^2 are +10% and +48% higher, respectively.

Table 1
EL characteristics of the OLEDs in Fig. 4a–c with and without the nRTL.

	At 3000 cd/m^2		At 100 mA/cm^2
	CE (fcd/Al)	PE (lm/W)	EOE (%)
Ref. [w/o nRTL]	2.39 (–)	0.54 (–)	0.96 (–)
Device A [interlayer]	3.32 (+39%)	0.82 (+51%)	1.05 (+10%)
Device B [nRTL]	3.85 (+61%) 1	10 (+102%)	1.42 (+48%)

( ): Enhancement ratios.

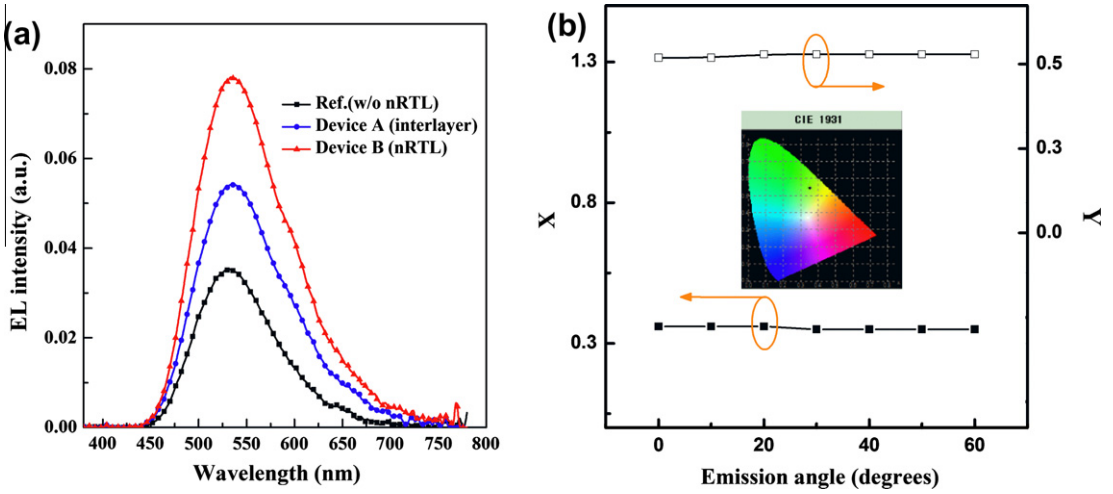

Fig. 5. (a) Emission spectra of device without nRTL (squares), device A (circles, with interlayer), and device B (triangles, with nRTL), measured from the surface normal at a current density of 100 mA/cm^2. (b) CIE color coordinate emission as function of angle for device B with the nRTL.

been optimized yet. Further investigation of optimization of the nanosized random patterns is ongoing.

Unlike the enhancement in PC OLEDs, which appears as sharp peaks [13], the enhancement in our devices with the nRTL appears over the entire EL spectrum. The EL spectra of the OLEDs at a current density of 100 mA/cm^2 are shown in Fig. 5a. The EL intensities of the devices A and B are increased by more than +52% and +104%, respectively, compared to the reference device without the nRTL. These data imply that the introduction of the out-coupling layer does not change the EL spectrum of the device. Moreover, the spectra for devices A and B show no variation with viewing angle (Figs. S1 and S2).

Fig. 5b shows the change in International Commission on Illumination (CIE) color coordinates with the emission angle in the device B. When the emission angle was increased from 0° to 60°, the CIE color coordinates of the device B changed from (0.3586, 0.5433) to (0.3518, 0.5453). The variations in the *x* and *y* color coordinates were 0.0068 (1.90%) and 0.002 (0.37%) in device B (Table S1).

4. Conclusion

In summary, we demonstrated a simple printing-process-based light out-coupling efficiency improvement technology for OLEDs and the nRTL. Compared to conventional devices without the nRTL, the power efficiency of OLEDs with the nRTL were greatly improved (+102%) at 3000 cd/m^2, and the improvement factor increased with increasing current density. Light generated in the OLEDs was dispersed by the nanosized structures of the nRTL and scattered in random directions. Moreover, the nRTL is free of the viewing-angle-dependent color distortion of the spectral shape and intensity that appears when previously reported techniques, including PCs, are used. Light trapped in the ITO anode and glass substrate is redirected toward the glass substrate and air by the nRTL, thereby enabling the extraction of the wave-guided light. The printing process was conducted at room temperature under an air atmosphere with high reproducibility and high uniformity at a large scale. The demonstrated technology has high potential for application to large-area mass production of OLED applications owing to its simplicity, high reproducibility, and uniformity.

Acknowledgments

This research was supported by the Basic Science Research Program through the National Research Foundation of Korea (NRF) funded by the Ministry of Education, Science and Technology (MEST) (CAFDC-20120000816), the NRF (No. 2012R1A6A3A04039396) Project of the MEST, and the IT R&D Program of MKE/KEIT (No. 2009-F-016-01, Development of Eco-Emotional OLED Flat-Panel Lighting). The authors thank the staff of KBSI for technical assistance.

Appendix A. Supplementary material

Supplementary data associated with this article can be found, in the online version, at http://dx.doi.org/10.1016/j.orgel.2012.10.009.

References

[1] P.E. Burrows, G. Bulovic, Z. Shen, S.R. Forrest, M.E. Thompson, IEEE 44 (1997) 1188–1203.
[2] Y. Xiong, W. Xu, C. Li, B. Liang, L. Zhao, J. Peng, Y. Cao, J. Wang, Org. Electron. 9 (2008) 533–538.
[3] H. Sasabe, J. Kido, Chem. Mater. 23 (2010) 621–630.
[4] B.W. D'Andrade, S.R. Forrest, Adv. Mater. 16 (2004) 1585–1595.
[5] H. Wu, G. Zhou, J. Zou, C.L. Ho, W.Y. Wong, J. Peng, Y. Cao, Adv. Mater. 21 (2009) 4181–4184.
[6] C. Adachi, M.A. Baldo, M.E. Thompson, S.R. Forrest, J. Appl. Phys. 90 (2001) 5048–5051.
[7] G. Gu, D.Z. Garbuzov, P.E. Burrows, S. Venkatesh, S.R. Forrest, Opt. Lett. 22 (1997) 396–398.
[8] C.F. Madigan, M.H. Lu, J.C. Sturm, Appl. Phys. Lett. 76 (2000) 1650–1652.
[9] S.R. Forrest, Org. Electron. 4 (2003) 45–48.
[10] I. Schnitzer, E. Yablonovitch, C. Caneau, T.J. Gmitter, A. Scherer, Appl. Phys. Lett. 63 (1993) 2174–2176.
[11] M. Fujita, T. Ueno, K. Ishihara, T. Asano, S. Noda, Appl. Phys. Lett. 85 (2004) 5769–5771.
[12] S. Jeon, J.W. Kang, H.H. Park, J.J. Kim, J.R. Youn, J. Shim, J.H. Jeong, D.G. Choi, K.D. Kim, A.O. Altun, S.H. Kim, Y.H. Lee, Appl. Phys. Lett. 92 (2008) 223307–223309.
[13] K. Ishihara, M. Fujita, I. Matsubara, T. Asano, S. Noda, Appl. Phys. Lett. 90 (2007) 111114–111116.
[14] A.O. Altun, S. Jeon, J. Shim, J.H. Jeong, D.G. Choi, K.D. Kim, J.H. Choi, S.W. Lee, E.S. Lee, H.D. Park, J.R. Youn, J.J. Kim, Y.H. Lee, J.W. Kang, Org. Electron. 11 (2010) 711–716.
[15] J.H. Jang, M.C. Oh, T.H. Yoon, J.C. Kim, Appl. Phys. Lett. 97 (2010) 123302–123304.
[16] T. Tsutsui, M. Yahiro, H. Yokogawa, K. Kawano, M. Yokoyama, Adv. Mater. 13 (2001) 1149–1152.
[17] Y. Sun, S.R. Forrest, Nat. Photon. 2 (2008) 483–487.
[18] S. Moller, S.R. Forrest, J. Appl. Phys. 91 (2002) 3324–3327.
[19] M.K. Wei, I.L. Su, Opt. Express. 12 (2004) 5777–5782.
[20] S.H. Eom, E. Wrzesniewski, J. Xue, Org. Electron. 12 (2011) 472–476.
[21] B. Riedel, I. Kaiser, J. Hauss, U. Lemmer, M. Gerken, Opt. Express 18 (2010) A631–A639.
[22] W.H. Koo, S.M. Jeong, F. Araoka, K. Ishikawa, S. Nishimura, T. Totyooka, H. Takezoe, Nat. Photon. 4 (2010) 222–226.
[23] J.H. Lee, J.S. Kim, J.S. Park, K.E. Lee, S.S. Han, K.B. Lee, J. Lee, Adv. Funct. Mater. 20 (2010) 2004–2009.
[24] J.S. Kim, J.B. Cho, B.G. Park, W. Lee, K.B. Lee, M.K. Oh, Biosens. Bioelectron. 26 (2010) 2085–2089.